Proceedings of the 9th U.S. National and 10th Canadian Conference on Earthquake Engineering
Compte Rendu de la 9ième Conférence Nationale Américaine et
10ième Conférence Canadienne de Génie Parasismique
July 25-29, 2010, Toronto, Ontario, Canada • Paper No 803

ACTIVE WEDGE ANALYSIS OF SEISMIC PRESSURES FOR RETAINED SLOPES

Jonathan W. Pease, Ph.D., G.E., P.E. [1] and Dylan Menes, S.E., P.E.[2]

ABSTRACT

The Mononobe-Okabe (M-O) equation, routinely used in retaining wall design, cannot always determine an active seismic pressure coefficient, particularly for walls retaining uphill slopes in areas of high seismic activity. This shortcoming occurs when the method determines a critical failure envelope shallower than the slope of the retained soil, and an infinitely-long wedge results. A force-equilibrium wedge analysis was developed to obtain active seismic pressures where the M-O equation was not successful for a short retaining wall to be constructed in an existing embankment in Reno, Nevada. The wedge active seismic pressure (WASP) analysis allows for computation of reduced dynamic active pressures considering a variety of beneficial factors, including the effects of embankment geometry and cohesion.

Introduction

The Mononobe-Okabe (M-O) equation is an accepted method for determining active seismic lateral earth pressure (active earthquake) coefficients for retaining wall design. This method, originally published in 1929, provides for an extension of the Mohr-Coulomb equation to include pseudo-static horizontal and vertical inertia on the sliding mass. The M-O equation has been adopted and presented by numerous sources and codes (e.g. AASHTO 2006) However, the M-O equation includes a square root term which will produce imaginary results whenever the term (φ-θ- β) is less than zero, where φ is the friction angle, θ is the seismic inertia angle, and β is the ground slope angle above the wall. An approximate interpretation is that the slip angle is shallower than the actual ground slope angle, so that the volume of the failure wedge increases infinitely. A plot showing retained slope angle, friction angle, and design acceleration for which M-O does and does not work is shown on Fig. 1. This limitation is trivial for design acceleration of less than 0.15g. However, this has an impact in areas with higher design accelerations, or where higher design accelerations are required by modern structural codes.

A number of studies and investigations have been performed to evaluate the validity and accuracy of the M-O equation however none of these studies has addressed the problem of imaginary results for backfill slopes. (Elms and Richards, 1990) and (Whitman, 1990) recommend the use of displacement design to obtain a seismic coefficient which is appropriate

[1] Geotechnical Engineer, Kleinfelder, 4835 Longley Lane, Reno NV 89502, jpease@kleinfelder.com
[2] Structural Engineer, Summit Engineering, 5405 Mae Anne, Reno NV 89523. dylan@geostructsparks.com

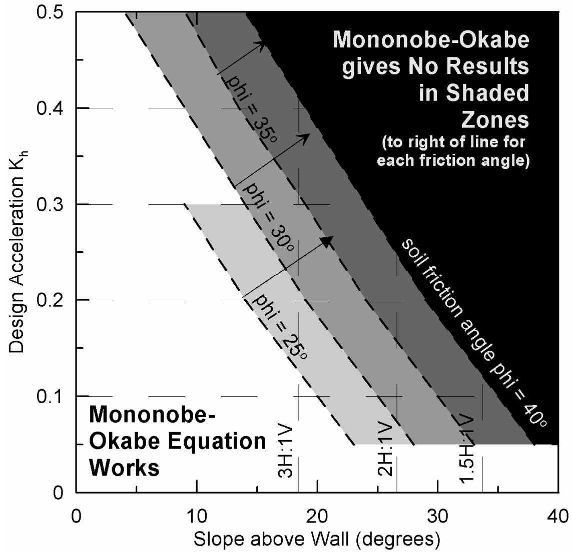

Figure 1. Design conditions for which the Mononobe-Okabe equation does not work

to the required seismic displacement performance of the wall, and which may reduce the design earthquake active pressure if moderate deformations are permissible. (Choudhury et al, 2006, Choudhury & Singh, 2006) investigated a pseudo-dynamic approach which closely approximates the results of M-O for the active condition. (Whitman 1990) points out that the pseudo-static approach is an engineering approximation which at best loosely shows the more complicated behavior of retaining systems under more complex modeling of seismic shaking.

In 2005, the author's firm was asked to prepare geotechnical recommendations for the Nevada Department of Transportation (NDOT) for a short retaining wall in Reno, Nevada. The proposed wall was to replace an existing wing wall retaining the edge of a 2H:1V slope under the US395/Plumb Lane bridge. The original conventional reinforced cantilever wall was to be removed due to roadway re-alignment, and be replaced with a wall oriented approximately 20 degrees further west of north. The new retaining wall is 14.3 m long and varies from 0 to 5.5 m high. The 2H:1V abutment fill above the retaining wall is retained at an oblique angle so that the average slope perpendicular to the wall is 3H:1V. The total embankment height to the level of the overlying freeway does not exceed 7.6m. The replacement wall was to be built with multiple rows of tie-backs with top-down construction due to the existing slope and to prevent any risk of settlement of the abutments for the overlying bridge.

Geotechnical exploration found medium dense to dense, well-graded gravel with sand and silt fill behind the existing walls which was placed as select borrow during original freeway construction in 1974. NDOT designs structures supported on or in select borrow using a friction angle of no more than 34 degrees with no cohesion, unless existing fills can be tested. The City of Reno is in an area of high seismic activity. Design of the retaining wall was by AASHTO design methods (AASHTO, 17th Edition, 2002), for a peak ground acceleration of 0.39 g. Because the proposed retaining wall was to be restrained using tie-backs, AASHTO design code required that the wall be designed for 1.5 times the peak ground acceleration, or 0.585 g. The M-O equation resulted in imaginary results for the Plumb Lane retaining wall. However, for the limited height of the wall and embankment, it seemed unlikely to be "undesignable."

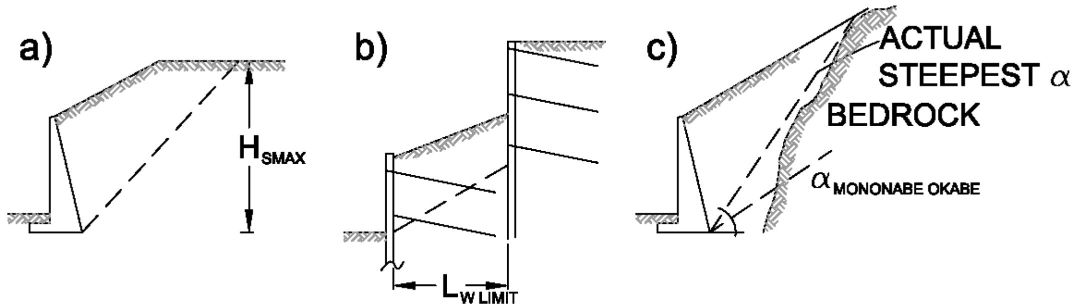

Figure 2. Practical retaining wall geometries for which M-O equation is conservative a) wall with limited slope height, b) wall with limited length of failure wedge, and c) wall with restricted failure angle.

Wedge Active Seismic Pressure Analysis

In order to justify a design for the Plumb Lane retaining wall, an equilibrium wedge analysis was developed which could better account for the actual wall and slope geometry. Several practical wall geometries where the M-O equation may produce imaginary or unconservative results are shown on Fig. 2. The M-O equation considers an infinite slope, whereas many retaining walls are built below embankment slopes of limited height (Fig. 2a). Walls may be surcharged by a slope of limited horizontal width, such as where a lower wall lies below an upper wall (Fig. 2b). Provided that the upper wall is fully anchored to avoid surcharging the lower wall, active seismic pressure on the lower wall should be lower due to the limited wedge length. In both of these cases, truncation of the failure wedge results in finite mass, and a real solution can be determined. Where walls are supporting a backfill zone against competent bedrock (Fig. 2c), the failure will potentially involve only the soil mass. A minimum failure angle may be present below which failure cannot occur (or at least failure cannot occur without increasing strength properties). The M-O equation only provides the active pressure at an optimum failure angle for a homogeneous soil mass. Lastly, even minor cohesion may considerably influence the active pressure. Cohesion is conventionally ignored for drained analysis of long-term conditions, but minor cohesion could be appropriate for seismic loading, which is very rapid by nature. Cohesion may be present due to soil dilative response (interlocking), dry cementation, capillary rise, or partially drained or undrained strength even for slightly-dirty granular soils.

The Wedge Analysis of Seismic Pressure (WASP) solution was initially developed using a spreadsheet to provide the minimum geometry and computation that would avoid infinite slopes and imaginary results. Any Culmann-type force-equilibrium analysis which allows multiple varied-slope elements should similarly overcome these limitations. WASP allows for inclusion of cohesion with or without tension cracks, a finite slope with a maximum slope height, and a maximum horizontal limit for failure. Surcharge loads can be investigated to see whether they extend the failure wedge. Both by design and of interest, the analysis is performed for all possible failure angles, to observe the distribution of active pressures for varying failure angles.

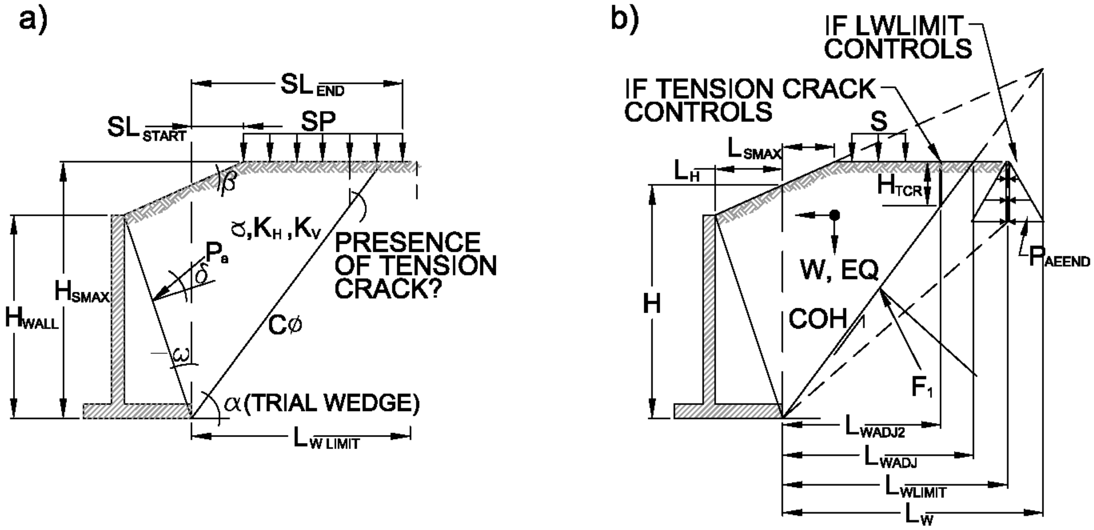

Figure 3. Geometry of wedge active analysis a) input parameters and b) derived geometry parameters

Fig. 3 summarizes the input and developed parameters used in the WASP solution. Most of these parameters match those required for the existing earth pressure solutions, while some are additional features in this analysis. These values include:

H_w = height of wall
H_{smax} = maximum height of slope to level bench
L_{wlimit} = horizontal limit of wedges (due to vertical obstruction or adjacent retaining wall)
c = soil cohesion
φ = soil friction angle

γ = soil unit weight
ω = back of wall angle from vertical (- orientation shown on Fig. 3)
β = Ground slope above top of wall
δ = wall/soil interface friction angle
K_h and K_v,= seismic coefficients
Use or omit tension crack
Surcharge pressure and start and end distance

Angles on Fig. 3 show positive rotation, except for the back of wall angle, ω, where the sign convention is positive for the wall surface sloping into the soil wedge (clockwise). The failure surface angle, α, is varied between 1 and 89 degrees to obtain solutions for all failure orientations. The horizontal and vertical seismic coefficients should be the actual values used for design. For example, for a peak ground acceleration of 0.4g, AASHTO/FHWA recommends multiplying the PGA (A) by 0.5 for non-restrained walls ($K_h = 0.5A$), so K_h would be entered as 0.20, not 0.40. Instead, the seismic design coefficients may be selected from displacement-based criterion (e.g Whitman, 1990; Elms and Richards, 1990).

The failure length from the heel of the wall is determined in several steps. If the wall-soil interface is not vertical, the soil height at the heel of the wall is determined as

$$H = H_w \cdot (1 - \tan(\omega) \cdot \tan(\beta)) \tag{1}$$

so that subsequent geometry and area calculations can be determined from a combination of right triangles and trapezoidal areas. The width of the triangle in front of the heel is

$$L_h = H_w \cdot \tan(\omega) \tag{2}$$

The horizontal distance to top of slope break is

$$L_{s\max} = (H_{s\max} - H)/\tan(\beta) \tag{3}$$

The depth of tension crack is

$$H_{tcr} = \frac{2 \cdot c \cdot \tan(45 + \phi/2)}{\gamma} \tag{4}$$

The failure length assuming an infinite slope is

$$L_w = H/(\tan(\alpha) - \tan(\beta)) \qquad \text{(for } \alpha > \beta\text{)} \tag{5}$$

For failure slopes shallower than or equal to the slope angle ($\alpha \leq \beta$), an arbitrarily large value of L_w is assumed. The adjusted length of failure including the maximum slope height is

$$L_{wadj} = \min[\langle H_{s\max}/\tan(\alpha)\rangle, \langle L_w \rangle] \tag{6}$$

Provided that the arbitrary value of L_w for $\alpha \leq \beta$ is sufficiently large, the adjusted failure wedge length will be controlled by the maximum slope height (the H_{smax} term), and the assumed arbitrary values of L_w will be eliminated from further analysis.

The failure length including tension cracks or a horizontal limit is more complex, because the location of the tension crack must be determined from the convergence of the slope angle, failure angle, and top of slope. The revised adjusted wedge length, L_{wadj2}, will depend on whether the tension crack or horizontal wedge limit is in front or behind the top-of-slope break:

$$L_{wadj2} = \min[\langle L_w - H_{tcr}/(\tan(\alpha) - \tan(\beta))\rangle, \langle L_{wadj} - H/\tan(\alpha)\rangle, \langle L_{w\lim it} \rangle] \tag{7}$$

If tension cracks are not permitted, this simplifies to L_{wadj}; if the failure wedge ends before the top of slope break and there is no tension crack, this simplifies to L_w. The height of the end of the failure wedge is

$$\begin{aligned}
H_{vend} &= H - L_{w\lim it}(\tan(\alpha) - \tan(\beta)) && \text{(if } L_{wadj2} \leq L_{smax} \text{ and } L_{wlimit} \text{ controls)} \\
H_{vend} &= (L_{wadj} - L_{w\lim it})/\tan(\alpha) && \text{(if } L_{wadj2} > L_{smax} \text{ and } L_{wlimit} \text{ controls)} \\
H_{vend} &= H_{tcr} && \text{(if controlled by tension crack)}
\end{aligned} \tag{8}$$

The soil volume and wedge mass can then be determined from a combination of simple geometric shapes. If the failure wedge intercepts the ground surface at or before the top of slope break ($L_{wadj2} \leq L_{smax}$), the wedge weight is largely trapezoidal, except for the triangular area above the wall heel. The weight is downward, thus the overall term is negative.

$$W = -\gamma \cdot L_{wadj2} \cdot \left(\frac{H + H_{tcr}}{2} \right) + \frac{\gamma \cdot L_h \cdot H}{2} \tag{9}$$

If the failure wedge intercepts the ground surface past the top of slope break, superposition of triangles is used.

$$W = -\frac{\gamma \cdot L_{wadj} \cdot H_{s\max}}{2} + \frac{\gamma \cdot Ls\max \cdot (H_{s\max} - H)}{2} + \frac{H_{vend}{}^2}{(2 \cdot \tan(\alpha))} + \frac{\gamma \cdot L_h \cdot H}{2} \tag{10}$$

Total cohesion on the failure plane is

$$COH = c \cdot \min\left(L_{wadj} / \cos(\alpha) /, L_{wadj2} / \cos(\alpha)\right) \tag{11}$$

Forces on the active wedge including cohesion along the slip plane, surcharge pressures, vertical and horizontal seismic inertial loads, can be determined from the geometric parameters. The required active forces for vertical and horizontal equilibrium are determined for all possible failure angles (α) from the following equations,

$$P_{av} = -\left[\frac{COH \cdot \sin(\alpha) + W \cdot (1 + k_v) + S + F_1 \cdot \cos(\alpha - \phi)}{\sin(\delta - \omega) + \dfrac{\cos(\alpha - \phi) \cdot \sin(\alpha + \omega - \delta)}{\cos(\phi)}} \right] \tag{12}$$

$$P_{ah} = \left[\frac{-COH \cdot \cos(\alpha) + W \cdot (k_h) + P_{aeend} + F_1 \cdot \sin(\alpha - \phi)}{\cos(\delta - \omega) - \dfrac{\sin(\alpha - \phi) \cdot \sin(\alpha + \omega - \delta)}{\cos(\phi)}} \right] \tag{13}$$

Where S is the vertical surcharge pressure, P_{aeend} is the active force on the end of the trapezoidal mass (described below), and F_1 is the force on the failure plane due to all the imposed forces except P_a:

$$F_1 = [-(W(1 + k_v) + S) \cdot \cos(\alpha) + (W \cdot k_h + Paeend) \cdot \sin(\alpha)] / \cos(\phi) \tag{14}$$

The largest of either the computed vertical or horizontal active pressures is used to determine the active or seismic active lateral earth pressure coefficient, K_a or K_{ae},

$$K_{a(ae)} = \frac{2 \cdot \max(P_{ah}, P_{av})}{\gamma \cdot H_w{}^2} \tag{15}$$

As formulated, the overall value of the seismic active pressure coefficient is determined over the whole wall height, not considering a reduction in wall height for a tension crack.

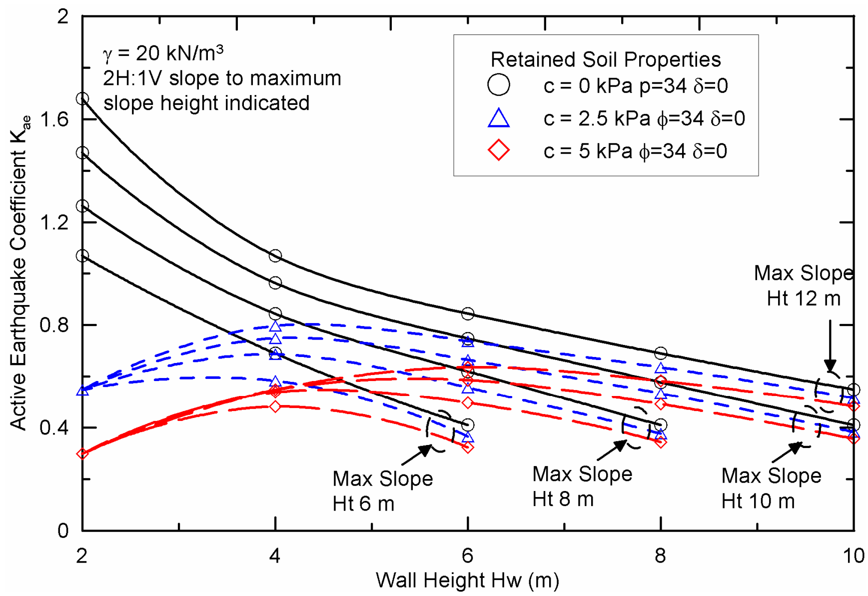

Figure 4. Typical results for variable wall height and cohesion (constant embankment height, soil properties, and horizontal coefficient)

Where a tension crack is considered, the pressure on the vertical crack at the back of the active wedge is zero. When the wedge length limit, L_{wlim}, is considered however, an active pressure surcharge, $P_{ae\ end}$, is applied to the uphill end of the failure wedge. The vertical boundary, which may represent an uphill wall tier, building wall, etc. (Fig. 2b), must be designed to be stable without additional support from or bearing on the active wedge of the lower wall. However, the soil wedge will impose active pressures against the stable boundary, and therefore to maintain equilibrium, the reaction to this active pressure is reflected as an external force on the failure wedge. The applicable slope angle is the opposite sign to the backfill slope surface angle ($\beta_{reflected} = -\beta$) or is level, depending on the location of the vertical boundary in front of or behind the top of slope, L_{smax}. Since the active force is in the opposite direction to the earthquake inertia at the instant of application, the active pressure is computed conservatively using the Coulomb equation (assuming a zero rather than negative seismic coefficient).

Evaluation of Typical WASP Results

WASP results are dependent on the actual wall geometry and dimensional parameters, and therefore cannot be readily normalized to dimensionless plots unless cohesion is set to zero. Typical results for a selected soil friction angle and variable soil cohesion, wall height, and maximum slope height are presented on Fig. 4, which would be appropriate for a 2 to 10m high semi-gravity wall in a 6 to 12 m high slope. All the solutions below except where the wall is the same height as the slope (level ground behind the wall at the embankment height) would be imaginary using M-O. It can be seen that the addition of even minor cohesion (2.5 kPa = 50 psf) the active earthquake pressure can be reduced moderately to significantly. The use of cohesion should be used only based on judgment by an experienced geotechnical practitioner. Using maximum slope height and horizontal limits set to large values, and zero cohesion, WASP accur-

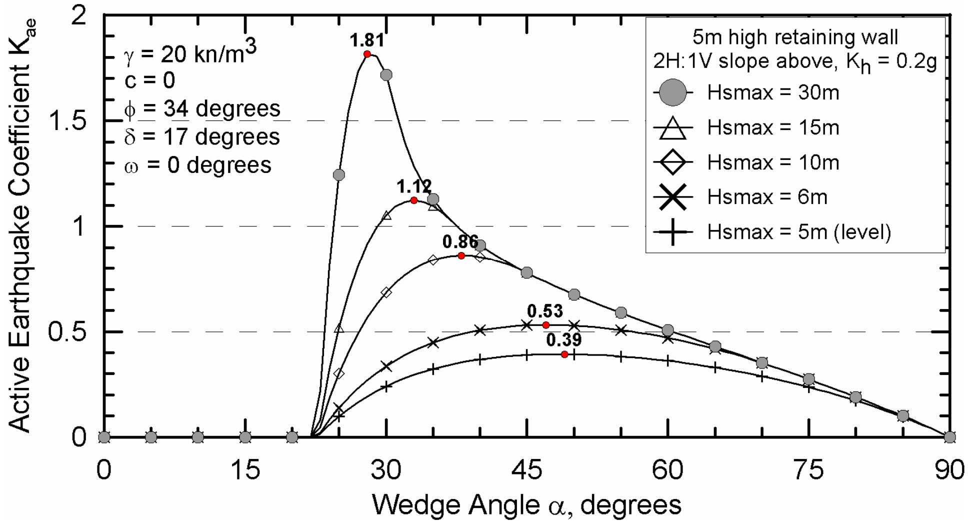

Figure 5. Variation of active seismic pressure coefficient with maximum slope height and wedge angle

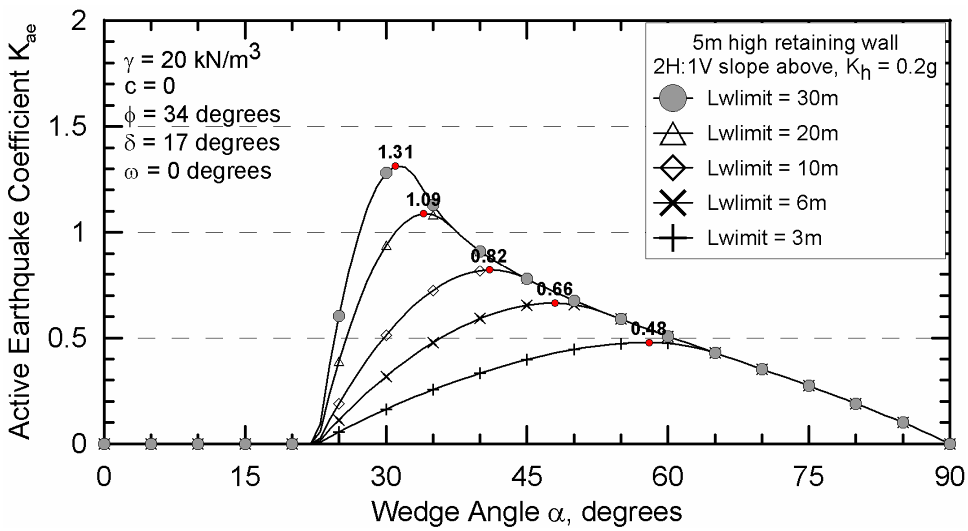

Figure 6. Variation of active seismic pressure coefficient with horizontal limit and wedge angle

-ately computes both Coulomb and non-imaginary M-O earth pressures. Other results can be confirmed using General Limit Equilibrium methods (Transportation Research Board, 2008).

It is instructive to observe the variation in active seismic pressure coefficient with trial angle. This is shown on Fig. 5 through 7 for a 5-m-high wall with a 2H:1V (26.6 degree) backfill slope surface and a horizontal seismic coefficient of 0.2g. The maximum values on each curve on Figs. 5 through 7 are the active seismic pressure coefficient.

Fig. 5 shows the variation in active seismic pressure for a range of maximum slope heights (5 to 30m) that are common for highway embankments. As the overall slope height seen increases to 30 m, the failure angle drops to near the slope angle and would become an infinite

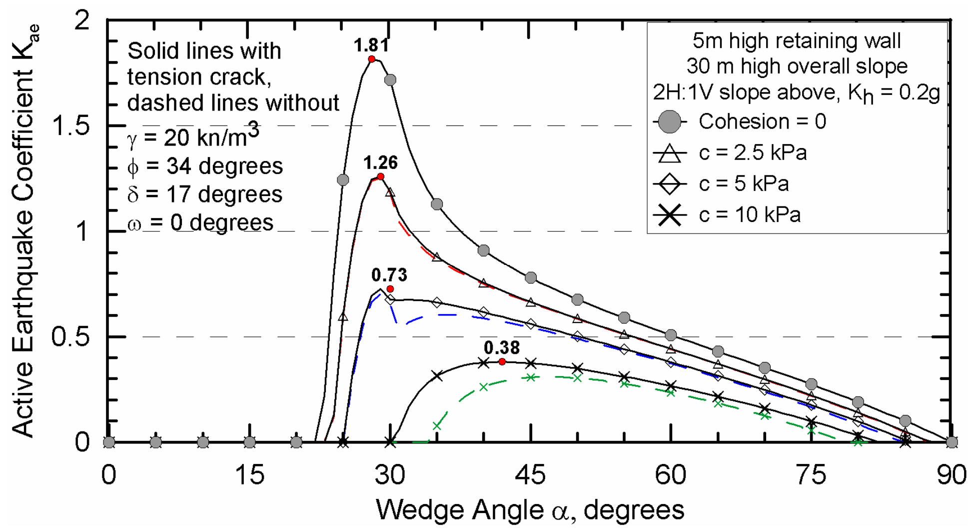

Figure 7. Variation of active seismic pressure coefficient with cohesion and wedge angle

failure wedge and infinite earth pressure if the slope height were not capped. This can be by the narrow band of peak results between 25 and 30 degrees for the 26.56-degree, 30-m slope. The solutions for each slope height converge to the same line at the angle where the failure plane intercepts the ground surface slope in front of the slope break. WASP results in the correct active pressure condition for level ground, 0.39, that can be determined from the M-O equation.

Fig. 6 shows the reduction in active seismic pressure as the result of imposing a horizontal limit to the failure wedge such as due to an adjacent uphill wall. It may be possible to add the uphill wall lateral force back to the earth pressure load on the lower wall.

Fig. 7 shows the variation in the active seismic coefficient for a 2H:1V slope with the inclusion of a small amount of cohesion. Even a small increase in cohesion of 2.5 to 10 kPa (50 to 200 psf) can potentially decrease the active seismic pressure to 20 to 40 percent of results without cohesion in critical cases where K_h is very high. Assuming worst saturation conditions and the earthquake do not coincide, this cohesion could possibly be provided by capillary pressures or minor cementation expected in a normal soil. Results on Fig. 7 shows that inclusion of a tension crack results in a higher K_{ae}, but K_{ae} is not substantially greater than without the tension crack. Therefore, it would be conservative, but not require excessive additional wall support to assume a tension crack develops.

One of the benefits of the WASP output is that both the maximum earth pressure and orientation and also alternative failure angles with only slightly lower earth pressure are presented. For a wall bounded by bedrock or other more competent materials shown on Fig. 2c, the failure surface below the angle of the rock interface potentially can be ignored to allow selection of a lower active earth pressure. For example, if the walls in Fig. 5 are located in front of a stable 1H:1V bedrock face, the active seismic pressure coefficient would not exceed 0.70 even for infinite retained height. The results also allow more thorough consideration of tieback anchor lengths which must develop their support behind the active seismic failure wedge. In

Fig. 5, all failure wedges steeper than 22 degrees could impose some active seismic failure pressure on the wall. Although for level ground (Kae = 0.39) the failure angle is 48 degrees, there is a range of slip surfaces as low as about 35 degrees that have nearly the same seismic influence as the critical slip surface, and could interact with the tieback bonded zone.

Design Example

Design of the Plumb Lane retaining wall used the following parameters at the maximum wall height: H_w = 5.5m, H_{smax} = 7.6m, β = 18.6º (3H:1V), ω = 0º, c = 13 kPa, φ = 34º, δ = 17º, γ = 20 kN/m^3, and K_h = 0.585g. The cohesion was back-analyzed from our judgment that the soil could be excavated in 1.6-m-vertical unsupported faces for shotcrete and tieback placement, which requires a short-term cohesion of at least 13 kPa. Active seismic pressures of 0.90 and 1.05 (at angle δ) were determined for maximum height and half-height; a horizontal active seismic pressure of 1.00 was selected for design. The failure angle for the maximum active seismic pressure varied between 17 and 24 degrees for the half-height and full-height walls, respectively, which allowed for determination of the required unbonded length of tiebacks.

Conclusions

WASP overcomes limitations of the M-O equation to determine active seismic pressure coefficient even for steep backfill slopes and high seismic accelerations. Inclusion of common slope features such as a maximum slope height, horizontal slope limits due to adjacent structures, cohesion, and other aspects can reduce the active seismic pressure coefficient, and optimize wall design. Calculation of active seismic pressure at each potential failure orientation allows insight into failure mechanisms and assures that alternate failure wedges are not neglected.

References

American Association of State Highway and Transportation Officials (AASHTO), 2006. *LRFD Bridge Design Specifications*, 4th Edition.

Choudhury, D. and S. Sing, 2006, New Approach for Determination of Static and Seismic Active Earth Pressure, *Geotechnical and Geological Engineering*, Vol 24(1), p. 117, Springer, Netherlands.

Choudhury, D., S. Nimbalkar, and J. Mandal, 2006. Comparison of Pseudo-Static and Pseudo-Dynamic Methods of Seismic Earth Pressure on Retaining Wall, *Journal of the Indian Geophysical Union*, Vol 110 No. 4. pp. 263 - 270.

Elms, D.G. and R. Richards, 1990, Seismic Design of Retaining Walls, Proceedings of *Design and Performance of Earth Retaining Structures*, Ithaca, New York, June 18 – 21, 1990, ASCE Geotechnical Special Publication No. 25., ASCE, Washington D.C.

Transportation Research Board, Seismic Analysis and Design of Retaining Walls, Buried Structures, Slopes, and Embankment, NCHRP Report 611, Washington D.C.

Whitman, R.V., 1990. Seismic Design and Behavior of Gravity Retaining Walls, Proceedings of *Design and Performance of Earth Retaining Structures*, Ithaca, New York, June 18 – 21, 1990, ASCE Geotechnical Special Publication No. 25. ASCE, Washington D.C.